Characteristics of Power and Cross Spectra of Wind Pressure Fluctuations on Dome-like Structures

Yuan-Lung Lo[a], Jun Kanda[a]

[a]*The University of Tokyo, 5-1-5 Kashiwinoha, Kashiwa, Chiba, Japan*

ABSTRACT: Experiments of four basic dome-like models were conducted for the wind pressure measurement. With the different ratios of height-to-span, characteristics of wind pressure fluctuations on the dome roofs can be categorized into three regions. It was indicated that different regions have different patterns of power and cross spectra. Therefore the wind loads may be evaluated with different contributions in three regions.

KEYWORDS: Dome-like, Wind pressure fluctuation, Cross correlation, Admittance function, Root-coherence function, phase function

1 INTRODUCTION

Dome-like roofs are most popular and constructed among large-scale structures. However, such kind of curved geometric design makes the estimation of wind loads a laborious task for wind engineers. Toy et al. (1983) showed that with the increased turbulent intensity, both separation and reattachment points move downstream. Ogawa et al. (1991) investigated the characteristics of power and cross spectra and proposed location-dependent approximated models. Uematsu (1997 & 2008) studied the statistical nature of wind pressure coefficients and proposed an evaluation system for the cladding design by neural network technique. This research intends to investigate the characteristics of power and cross spectra on the dome roof. Wind pressure coefficients are calculated for the zoning of dome roofs. Power and cross spectra in each region are presented to show different patterns. Another aim of this research is to indicate that a uniform pattern of spectral characteristics may be insufficient for the estimation of wind loads.

2 EXPERIMENT DESIGN

Wind pressure measurements were conducted in a boundary layer wind tunnel with a 12.0m (length) × 2.0m (width) × 1.8 (height) dimensions. A turbulent boundary layer flow similar to suburban terrain with power law index equals to 0.27 was used. Figure 1 shows the picture of the setup of the wind tunnel. Figure 2 shows the profiles of mean wind velocity and turbulence intensity. Table 1 shows the combinations of the models. Pressure taps are installed along the meridian and other two parallel lines in an equally 50mm interval. The coordinate dimensions and the labeling of acrylic model are shown in Figure 3. Wind speed of 10 m/sec at boundary layer height, 1200mm, was fixed and the turbulence intensity varied from 18% to 24% at the model height. Four corresponding Reynolds numbers of model heights are in the range of 0.91×10^5~1.28×10^5.

Table 1 Testing model

	f/D=0.2	f/D=0.5
h/D = 0.0	A0	D0
h/D = 0.2	A2	D2

Figure 1 Setup of wind tunnel

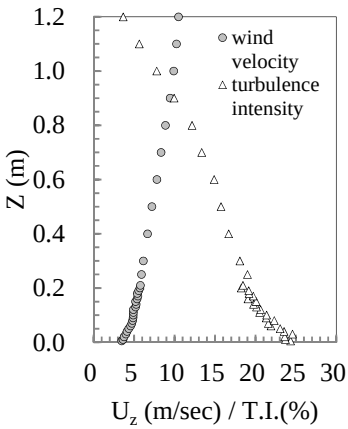

Figure 2 Profiles of turbulent flow

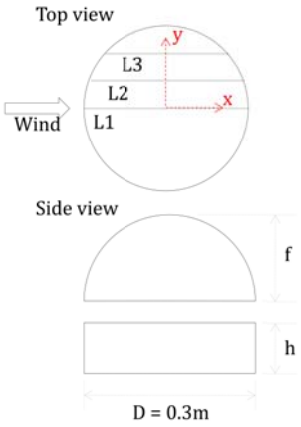

Figure 3 Labeling of acrylic models

3 WIND PRESSURE DISTRIBUTIONS

All pressure measured are normalized by velocity pressure at the model height as defined by Equation 1.

$$C_{p,i} = \frac{P_i - P_{ref}}{0.5\rho U_H^2} \quad (1)$$

where P_i = *i-th* dynamic pressure; P_{ref} = reference pressure at model height; ρ = air density; U_H = wind velocity at model height. Figure 4 shows the distributions of mean pressure coefficients. For A0 and A2, positive values can be observed in the frontal and rear part in L1 and L2. The increase of h/D results in the downward shifting of distribution in A2 model. For D0 and D2, only the frontal part of L1 and L2 shows the positive pressure, meanwhile, the rear part shows a flat distribution. L3 in both models shows a similar distribution to that in A0 and A2.

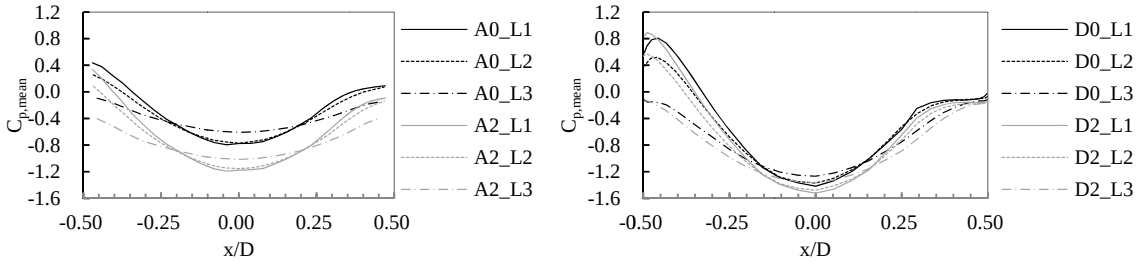

Figure 4 Mean pressure coefficient distributions

Cross correlations between two adjacent pressure fluctuations, $R_{i,i+1}$, are calculated in Figure 5. In A0 and A2, the lowest correlation occurs in the rear part of L1 and L2. The lowest point is earlier in A0 than that in A2. In D0 and D2, the lowest point seems occur at the same position in the rear part of L1 and L2. Comparing four models, it can be observed that the increase of f/D results in relatively large occurrence of lower cross correlation.

From the mean pressure coefficients and the correlation between two adjacent pressure fluctuations, three regions can be preliminarily assumed to present different pattern of wind flows. Region 1 is assumed as the frontal part up to x/D=-0.45 for A0 and -0.35 for D0. Region 3 is assumed as the rear part begins from x/D=0.4 for A0 and 0.3 for D0. Region 2 is between Region 1

and 3. For Region 1, the pressure fluctuation is affected directly by the wind velocity fluctuation of approaching wind so that positive values are observed. For Region 3, the lowest point of cross correlation may represent the separation point of wind flow. After the separation point, wakes are formed and the pressure fluctuations become less significant.

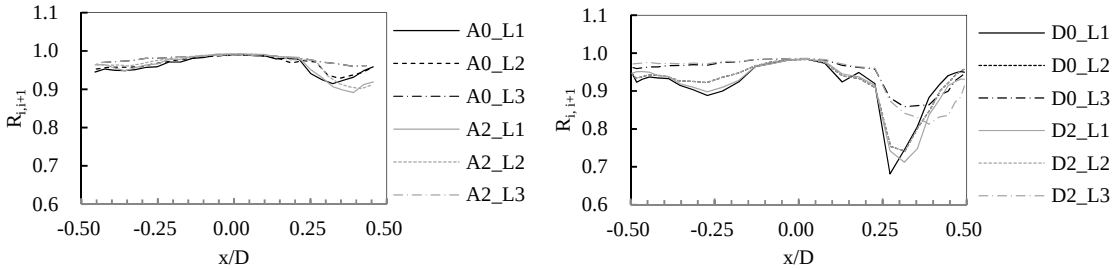

Figure 5 Cross correlation coefficients of two adjacent pressure fluctuations

4 POWER AND CROSS SPECTRA IN THREE REGIONS

The admittance function is defined by Equation 2 where $S_p(f)$ = power spectra of pressure fluctuation; $S_{UH}(f)$ = power spectra of wind velocity at model height.

$$\left|\chi(f)\right|^2 = \frac{S_p(f)}{\rho^2 U_H^2 S_{U_H}(f)} \qquad (2),$$

$$S_{p,i,i+1}(f) = \rho^2 \cdot U_H^2 \cdot \sqrt{\chi_i(f)\chi_{i+1}(f)} \cdot S_{U_H}(f) \cdot r_{i,i+1}(f) \cdot e^{i\theta(f)} \qquad (3)$$

Figure 6 shows different patterns of admittance functions in each region along L1 in D0 model. From Region 1 to Region 3, it is observed that the energy in the lower frequency range is decreasing and increasing in the higher frequency range. The pattern in Region 1 is similar to that of the approaching wind and Region 3 is considered being affected by the higher frequency of vortex after the separation.

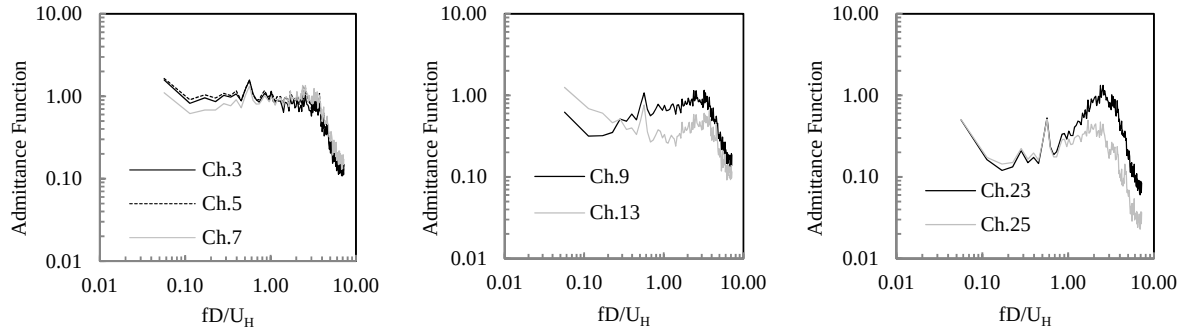

(a) Region 1 (b) Region 2 (c) Region 3

Figure 6 Admittance function in three regions

Cross spectra between pressure fluctuations at position i and i+1 can be approximated by Equation 3 where $r_{i,i+1}(f)$ = root-coherence; $\theta(f)$ = phase.

Figure 7 shows the root-coherence and Figure 8 shows the phase between two adjacent pressure fluctuations along L1 in D0 model. Region 1 and 3 has rather scatter distribution than Region 2. Studies in the past suggest a uniform pattern of root coherence and phase function for any location of the dome roofs. However, results in Figure 7 and 8 shows that since root-coherence

and phase functions are location-dependent, cross spectra should be calculated based on different locations of the dome roof.

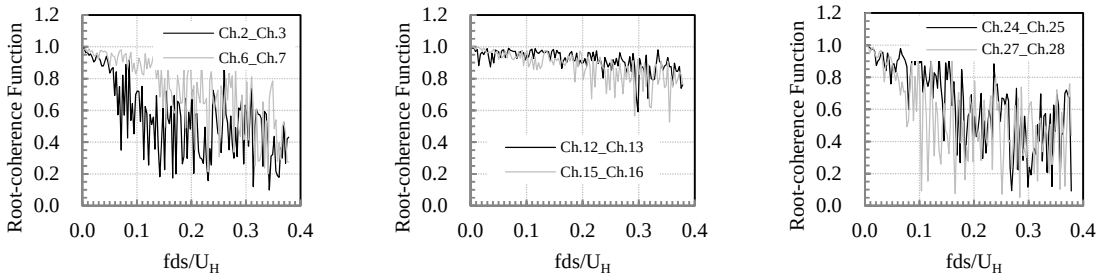

(a) Region 1 (b) Region 2 (c) Region 3

Figure 7 Root coherence function in three regions

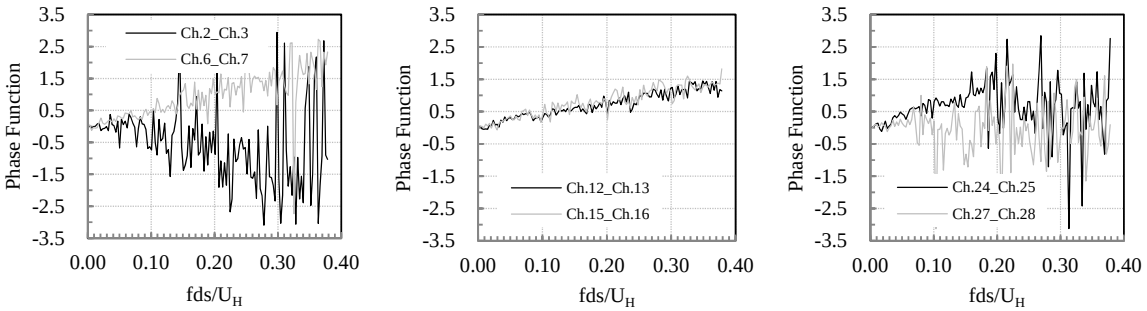

(a) Region 1 (b) Region 2 (c) Region 3

Figure 8 Phase function in three regions

5 CONCLUSIONS

The effects of f/D and h/D are investigated by observing wind pressure coefficients. Zoning of wind flow patterns on the dome roof is discussed based on wind pressure coefficients and cross correlation between two adjacent pressure fluctuations. Different regions show the location-dependent characteristics of pressure fluctuations and further indicate that a uniform flow pattern for any location of the dome roof may be insufficient for the estimation of wind loads in the future studies.

6 REFERENCES

1. C. M. Cheng, C. L. Fu, Characteristics of wind loads on a hemispherical dome in smooth flow and turbulent boundary layer flow, J. Wind Eng. Ind. Aerodyn. 98(2010), 328-344.
2. T. Ogawa, M. Nakayama, S. Murayama, Y. Sasaki, Characteristics of wind pressure on basic structures with curved surfaces and their response in turbulent flow, J. Wind Eng. Ind. Aerodyn. 38(1991), 427-438.
3. N. Toy, W. D. Moss, E. Savory, Wind tunnel studies on a dome in turbulent boundary layers, J. Wind Eng. Ind. Aerodyn. 11(1983), 201-212.
4. Y. Uematsu, M. Yamada, A. Inoue, T. Hongo, Wind loads and wind-induced dynamic behavior of a single-layer latticed dome, J. Wind Eng. Ind. Aerodyn. 66(1997), 227-248.
5. Y. Uematsu, R. Tsuruishi, Wind load evaluation system for the design of roof cladding of spherical domes, J. Wind Eng. Ind. Aerodyn. 96(2008), 2054-2066.